Genome-wide identification of *MAPKKK* genes and their responses to phytoplasma infection in Chinese jujube (*Ziziphus jujuba* Mill.)

ZhiGuo Liu
Agricultural University of Hebei
Lixin Wang
Agricultural University of Hebei
Chaoling Xue
Agricultural University of Hebei
Yuetong Chu
Agricultural University of Hebei
Weilin Gao
Agricultural University of Hebei
Yitong Zhao
Agricultural University of Hebei
Jin Zhao
Agricultural University of Hebei
Mengjun Liu (lmj1234567@aliyun.com)

Research article

Keywords: Chinese jujube, MAPKKKs, Jujube witches' broom, Phytoplasma, Expression profiles

Posted Date: January 22nd, 2020

DOI: https://doi.org/10.21203/rs.2.9872/v4

Version of Record: A version of this preprint was published at BMC Genomics on February 10th, 2020. See the published version at https://doi.org/10.1186/s12864-020-6548-6.

Abstract

Background: Mitogen-activated protein kinase (MAPK) cascades play vital roles in signal transduction in response to a wide range of biotic and abiotic stresses. In a previous study, we identified ten *ZjMAPKs* and five *ZjMAPKKs* in the Chinese jujube genome. We found that some members of *ZjMAPKs* and *ZjMAPKKs* may play key roles in the plant's response to phytoplasma infection. However, how these *ZjMAPKKs* are modulated by *ZjMAPKKKs* during the response process has not been elucidated. Little information is available regarding *MAPKKKs* in Chinese jujube.

Results: A total of 56 *ZjMAPKKKs* were identified in the jujube genome. All of these kinases contain the key S-TKc (serine/threonine protein kinase) domain, which is distributed among all 12 chromosomes. Phylogenetic analyses show that these *ZjMAPKKKs* can be classified into two subfamilies. Specifically, 41 *ZjMAPKKKs* belong to the Raf subfamily, and 15 belong to the MEKK subfamily. In addition, the *ZjMAPKKKs* in each subfamily share the same conserved motifs and gene structures. Only one pair of *ZjMAPKKKs* (15/16, on chromosome 5) was found to be tandemly duplicated. Using qPCR, the expression profiles of these *MAPKKKs* were investigated in response to infection with phytoplasma. In the three main infected tissues (witches' broom leaves, phyllody leaves, and apparently normal leaves), *ZjMAPKKK26* and *-45* were significantly upregulated, and *ZjMAPKKK3, -43* and *-50* were significantly downregulated. *ZjMAPKKK4, -10, -25* and *-44* were significantly and highly induced in sterile cultivated tissues infected by phytoplasma, while *ZjMAPKKK6, -7, -17, -18, -30, -34, -35, -37, -40, -41, -43, -46, -52 and -53* were significantly downregulated.

Conclusions: For the first time, we present an identification and classification analysis of *ZjMAPKKKs.* Some *ZjMAPKKK* genes may play key roles in the response to phytoplasma infection. This study provides an initial understanding of the mechanisms through which *ZjMAPKKKs* are involved in the response of Chinese jujube to phytoplasma infection.

Background

Mitogen activated protein kinase (MAPK) cascades comprise three specific kinase families: MAP kinase kinase kinases (MAPKKKs), MAP kinase kinases (MAPKKs) and MAP kinases (MAPKs). Essentially, these kinase families are intermediate signalling modules that operate between signal sensing and the activation of related transcription factors. These kinases are involved in plant responses to biotic and abiotic stresses, such as drought, salinity, cold and pathogen attack [1-3]. The conserved serine/threonine MAPKKKs can be activated by plasma membrane receptors which, in turn, phosphorylate MAPKKs, which then activate MAPKs by sequential phosphorylation. Finally, MAPKs regulate other kinases or related transcription factors in response to various stresses [4, 5]. Each MAPK cascade family consists of a number of members, and the number of members varies significantly between families. For example, the MAPKKK family comprises a greater number of members and shows more complex sequence diversity than the other two families. The members belonging to the MAPKKK family can be classified into the subfamilies Raf, ZIK and MEKK according to their characteristic sequence motifs [6]. Structural diversity is found among MAPKKKs in each subfamily. The Raf subfamily has a C-terminal kinase domain and a long N-terminal regulatory domain, while ZIK proteins have only N-terminal kinase domains, and the MEKK subfamily has fewer conserved kinase

domains. In addition, a long N-terminal regulatory domain forms the backbone for the Raf and ZIK subfamilies [1, 6].

MAPK cascades have been implicated in signal transduction in distinct innate immunity [7, 8]. In *Arabidopsis*, the *MEKK1-MKK4/5-MPK3/6-WRKY22/WRKY29/FRK1* cascade is involved in innate immunity signal transduction, and the *MEKK1-MKK1/MKK2-MPK4* kinase cascade can negatively activate *MEKK2,* which further leads to SUMM2-mediated immune responses [9, 10]. In tobacco, *NPK1-MEK1-Ntf6* can regulate *WRKY/MYB* transcription factors to participate in the tobacco mosaic virus infection pathway [11]. In addition, the *MAPKKKα-MKK2/MKK4-MPK2/MPK3* cascades participate in the Pto-mediated effect or triggered immunity (ETI) pathway by regulating the transcription factor *TGA* in tomato [12]. Hence, the MAPK pathway is indeed involved in the response to pathogen attack and may also play essential roles in the response to phytoplasma infection in Chinese jujube.

The *MAPKKK* family has now been characterised in the plant kingdom. A total of 80 *MAPKKKs* were first identified in *Arabidopsis* in 2002 [6, 13]. In the following years, an array of different *MAPKKKs* have been identified in a range of plant species, including rice (75 members), *Zea mays* (71 members), *Vitis vinifera* (45 members), *Malus domestica* (72 members) and *Musa nana* (77 members) [14-17]. However, little is known about the biological information and function of the *MAPKKK* gene family in Chinese jujube, even though detailed information for *ZjMAPKKs* and *ZjMAPKs* has previously been reported by our group [18].

Jujube witches' broom disease (JWB) is caused by '*Candidatus Phytoplasma* ziziphi'. JWB is a devastating disease in Asia [19]. Since the 1990s in China and with no effective control methods, JWB disease has severely impacted yields of Chinese jujube [20]. Our group has focused on this disease for many years, and we have published a book, 'Jujube Witches' Broom Disease', which provides detailed information on a number of key questions, including how the phytoplasma infects the plant with a one-year life cycle, how to test for JWB and how to evaluate the severity of JWB. Typical symptoms that can be observed in a plant suffering phytoplasma disease include witches' broom and phyllody. The physiological and biochemical behaviours of jujube plants infected by this phytoplasma have been widely studied [20, 21, 22], but the underlying molecular mechanisms have not been elucidated. Recently, MAPKs have been reported in response to phytoplasma infection of Chinese jujube with analysis of their expression levels in different phytoplasma-infected materials [23]. This study has provided valuable insights into the important roles played by MAPKs during the infection process. In addition, *ZjMPK2*, *ZjMKK2* and *ZjMKK4* have been shown to be the main genes involved in the Chinese jujube-phytoplasma interaction. Additionally, using yeast two-hybrid analyses, it has been demonstrated that ZjMKK2 interacts with ZjMPK2 [18, 24]. All these results demonstrate the important function of MAPK cascades in response to phytoplasma infection in Chinese jujube. However, identification and initial functional analyses of *ZjMAPKKKs* are needed to build our knowledge of the complete MAPK cascade signalling transduction pathway. Thus, the aim of this study was to identify *ZjMAPKKKs* using genome-wide and phylogenetic analyses to predict the gene structure and conserved motifs of *ZjMAPKKKs*. Then, the expression profiles of these *ZjMAPKKKs* in response to phytoplasma infection were investigated by qPCR. The end goal is to expand our understanding of the mechanism through which *ZjMAPKKKs* are involved in the defence responses of Chinese jujube to witches' broom disease.

Method

Identification of *ZjMAPKKKs* in Chinese jujube

The *ZjMAPKKKs* gene family was identified according to our previous study on the identification of *ZjMAPKKs* and *ZjMAPKs* with some modifications [18]. First, the whole protein sequences of *MAPKKKs* in *Arabidopsis* were retrieved from TAIR databases **(Additional file 1)**. These sequences were used as queries to search against the whole jujube genome database (accession JREP00000000) [25]. In addition, the alignments of all *Arabidopsis MAPKKK* sequences were used to construct an HMM profile (http://hmmer.org/download.html) to search for other potential *MAPKKK* members in the jujube genome database. All the potential *ZjMAPKKK* genes that contain a protein kinase domain (PF00069) were confirmed by HMMER tools [26], redundancy was removed, and the remaining sequences were identified as belonging to the *ZjMAPKKK* family. Furthermore, the ExPASy Proteomics Server (http://expasy.org/) was used to calculate the theoretical pI (isoelectric point) and Mw (molecular weight) of the putative *ZjMAPKKKs* [27].

Gene structure, protein domain and motif analyses of *ZjMAPKKK* genes

The open reading frames (ORFs) of 56 *ZjMAPKKKS* were analysed through the National Center for Biotechnology Information (NCBI, http://www.ncbi.nlm.nih.gov) ORF finder, and the main protein domains of *ZjMAPKKKs* were also recorded by blastp of NCBI **(Additional file 2)**. GSDS (Gene Structure Display Server, http://gsds.cbi.pku.edu.cn/) was used to determine the exon/intron structures of individual *ZjMAPKKKs* by aligning the cDNA sequences with their corresponding genomic DNA sequences [28]. The MEME database was used to identify the conserved motifs of *ZjMAPKKKs* [29]. The ideal motif widths were set to between 6 and 50, and each protein sequence of the *ZjMAPKKKs* subfamily was used to determine the highest number of conserved domains [30].

Sequence alignment, phylogenetic and gene duplication analysis

All the protein sequences of *ZjMAPKKKs* were aligned by ClusterX software using the default parameter values. The alignments of the protein sequences of 56 *ZjMAPKKKs* and 80 *AtMAPKKKs* were then subjected to phylogenetic analysis using MEGA 6.06 alignment explorer. The parameters of alignment were as follows: gap opening penalty, 10.00; gap extension penalty, 0.50 (both in pairwise alignment and in multiple alignment); protein weight matrix, gonnet; residue-specific penalties, on; hydrophilic penalties, on; gap separation distance, 0; end-gap separation, on; use negative matrix, off; and delay divergent cutoff (%), 30. Phylogenetic trees were constructed by the neighbour-joining (NJ) method. The parameters of the constructed trees were as follows: statistical method, neighbour-joining; scope, all selected taxa; test of phylogeny, bootstrap method; number of bootstrap replications, 1000; substitution types, amino acid; model/method, Poisson model; rates among sites, uniform rates; pattern among lineages, same (homogeneous); and gaps/missing data treatment: complete deletion. The Multiple Collinearity Scan toolkit (MCScanX) was used to analyse the gene duplication events, with the default parameters and the homologous relationships being drawn using Circos software [31, 32].

Plant materials and treatments

Ziziphus jujuba Mill. 'Dongzao' was cultivated in the Experimental Station of Chinese Jujube, Hebei Agricultural University and used for experimental material. For each time point, leaf samples were collected from at least three healthy jujube trees and from three trees infected with JWB. All experimental trees were cultivated under natural environmental conditions [20, 22]. Each year, visual symptoms of JWB, such as phyllody leaves (floral organs becoming leaf-like, middle severity) and apparently normal leaves (infected but asymptomatic, or exhibiting minimal symptoms), were first observed in early June. Later, witches' broom leaves (shoots with small leaves, maximum severity) were observed in the middle of June. Finally, mature witches' broom leaves, phyllody leaves and apparently normal leaves were collected from the same branch of diseased trees in June, July, August, and September (on the 15^{th} day of each month). The leaves from healthy trees were used as controls for each time point. The use of the above time course is that the phytoplasma content of the branches increased dramatically during the period, reaching a peak in July and August and declining thereafter [20]. The different types of materials are shown in **Additional file 3.** Detection of JWB phytoplasma in the infected materials employed DAPI staining at the histological level and quantitative real-time PCR analysis (qRT-PCR) at the molecular level [22]. Each material was sampled with three replicates, one from each of three different trees. In addition, sterile cultivated JWB diseased plantlets of *Ziziphus jujuba* Mill. 'Goutouzao' were used as a parallel testing group, with healthy plantlets being used as controls (as shown in **Additional file 4**). The presence of JWB phytoplasma in the diseased and healthy sterile cultivated plantlets was detected using DAPI staining at the histological level (**Additional file 5**) [24]. Ten plantlets were pooled to form one sample, and three independent biological replications were sampled separately. All samples were frozen rapidly in liquid nitrogen and held at -80 °C pending RNA isolation and qPCR analyses.

RNA extraction and qRT-PCR analyses

Total RNA was extracted from the leaves using the TIANGEN RNA Extraction Kit. Genomic DNA contamination was removed by digestion with DNase. cDNA synthesis was carried out with the TaKaRa RNA PCR Kit (AMV) Ver. 3.0 (TaKaRa) according to the manufacturer's protocol using 1 μg of RNA template.

qRT-PCR was carried out on the Bio-Rad iQ™ 5 using TransStart Top Green qPCR SuperMix AQ131 (TransGen Biotech, China). The 20-μL reaction system contained 10 μL of 2×SYBR Premix ExTaq™, 0.4 μL each of 10 μM primers, 1 μL diluted cDNA and 8.2 μL ddH_2O. The thermal profile was preincubated for 3 min at 94°C followed by 40 cycles of 5 s at 94°C, 15 s at 55~63°C and 15 s at 72°C. Relative expression levels of *ZjMAPKKKs* were calculated by the $2^{-\Delta\Delta Ct}$ method [31] using *ZjActin* as an endogenous control for normalisation [32]. The primer sequences of *ZjMAPKKKs* for qPCR are shown in **Additional file 6**.

Heatmap construction

The expression profiles of all *ZjMAPKKKs* in the different samples are illustrated by a colour gradient heatmap. The heatmap was constructed by heatmap software Heml 1.0 using log2-based expression fold changes.

Statistical analyses

All data were analysed by the two-sample t-test method using Origin 8.0 software with range tests ($P<0.05$ and $P<0.01$).

Results

Genome-wide identification of *ZjMAPKKKs*

A total of 56 *ZjMAPKKKs* were defined. All of these kinases have the key S-TKc (serine/threonine protein kinase) domain and other conserved protein kinase domains (**Additional file. 2**). To clearly understand and discriminate between the *MAPKKK* genes, the locus of *ZjMAPKKKs* was designated according to the nomenclature suggestions for *Arabidopsis,* where *Zj* refers to *Ziziphus jujuba*, and the series numbers *ZjMAPKKK1-56* are coded in terms of their chromosome locations (**Table 1**). The *ZjMAPKKKs* are distributed over all 12 pseudochromosomes, except for *ZjMAPKKK44-56,* which could not be matched to a corresponding chromosome.

Specific information for each CDS and amino acid sequence of the *ZjMAPKKKs* is listed in **Additional files 1 and 7**. Based on the specific conserved signature motif, all the *ZjMAPKKKs* could be grouped into one of the two subfamilies Raf and MEKK. No ZIK subfamily members were identified. As shown in **Table 1**, the length of the CDS sequences ranged from 762 bp (*ZjMAPKKK36*) to 4455 bp (*ZjMAPKKK7*) with an average length of 1804 bp. The amino acid sequence length of ZjMAPKKKs varied from 253 (*ZjMAPKKK36*) to 1,484 (*ZjMAPKKK7*) amino acids (aa); the average length was 600 aa. The predicted molecular weight (Mw) of these proteins ranged from 28.29 (*ZjMAPKKK36*) to 160.66 (*ZjMAPKKK7*), and the theoretical isoelectric points (pI) ranged from 4.78 to 9.34.

Phylogenetic analyses of *ZjMAPKKK* genes

To assess the phylogenetic relationships between Chinese jujube and *Arobidopsis*, a phylogenetic tree was constructed with all 136 protein sequences (56 ZjMAPKKKs and 80 AtMAPKKKs). As illustrated in **Fig. 1**, the members of AtMAPKKKs could be clustered into three categories, Raf, ZIK and MEKK, indicating that the method used to build the phylogenetic tree was reliable. However, the 56 members of ZjMAPKKKs could be clustered into only two subfamilies, Raf and MEKK. In addition, the largest Raf subfamily consisted of 41 members, with the remaining 15 members of ZjMAPKKKs belonging to the MEKK subfamily. None could be ascribed to the ZIK subfamily. Moreover, some ZjMAPKKKs located on the same chromosome showed little divergence but clustered into the same group. Examples are ZjMAPKKK36, -37 and -40; ZjMAPKKK15 and -16; and ZjMAPKKK38 and -39. These results indicate that some duplication of ZjMAPKKKs occurred during the evolution of jujube.

Conserved domains and gene structure analyses of *ZjMAPKKKs*

Within the analysis of MEME software, five main conserved motifs were identified in all 56 ZjMAPKKKs (**Fig. 2**). Motifs 1, 3 and 4 were found in all ZjMAPKKKs, while the other two motifs were observed in all Raf subfamily members. The MEKK subfamily members fell into two groups: one contained motifs 1-4, including ZjMAPKKK21, -56, -6, -31, -10 and -25. The remaining members contained only motifs 1, 3 and 4. These

results illustrate that ZjMAPKKKs share the same conserved motifs, which further indicates that the protein structures for each subfamily are highly conserved.

For the analyses of the exon/intron contents, the differences among *ZjMAPKKKs* were significant. As shown in **Fig. 3** and in **Additional file 8**, the number of exons in *ZjMAPKKKs* ranged from 1 (*ZjMAPKKK9, -12, -29, -35, -36, -44* and *-54*) to 19 (*ZjMAPKKK42*). Interestingly, the members of *ZjMAPKKKs* containing only 1 exon all belong to the MEKK subfamily (47%). The highest number of exons in this subfamily was 17 (*ZjMAPKKK25* and *-10*), and the average number was 5.6. This result demonstrates that in this subfamily, significant loss and gains of exons took place during evolution. For the Raf subfamily, the number of exons varied from 2 (*ZjMAPKKK16* and *-28*) to 19 (*ZjMAPKKK42*) with an average number of 9.56. Although there was significant variation in the number of exons in the Raf and MEKK subfamilies, some exon structure patterns were clearly conserved in close paralogues. For instance, *ZjMAPKKK24* and *-49* have 12 exons, while *ZjMAPKKK37* and *-40* have 2 exons, and they are all closely clustered in the same phylogenetic tree. Collectively, the evolutionarily different organisations of the *ZjMAPKKK* gene structures between the Raf and MEKK subfamilies indicate that tandem and segmental duplication events may have occurred in ancient times and that diverse exon structures may function differently in the jujube genome.

Furthermore, with the multiple protein alignment of *ZjMAPKKKs*, the Raf-specific signature motif GTXX(W/Y)MAPE was found in the Raf subfamily, and the kinase domain was located at the N terminal or C terminal. In contrast, the less conserved MEKK-specific signature motif G(T/S)PX(W/F)MAPEV was observed in the MEKK subfamily, while the kinase domain was located at three positions: the N- or C-terminal or the central part of the proteins (**Fig. 4**). The features of the signature motifs of ZjMAPKKKs are consistent with other orthologues in other plant species, where they fulfil important roles in a diversity of signal transduction processes.

Synteny analysis of *ZjMAPKKK* genes

Tandem duplication events were first analysed according to the principle that two or more genes can be located on a chromosomal region within 200 kb [34] of one another. As shown in **Fig. 5**, one pair of *ZjMAPKKKs* (15/16) was the only tandem duplication event on LG5. In addition, 13 segmental duplication events with 22 *ZjMAPKKKs* were also identified. These results indicate that some *ZjMAPKKKs* may have been generated by gene duplication and that segmental duplication events were probably a major driving force in *ZjMAPKKK* evolution.

Phytoplasma detection in different tissues infected by phytoplasma

To characterize the functions of *ZjMAPKKKs* involved in phytoplasma infection, the expression levels of individual *ZjMAPKKKs* were detected by qPCR in two kinds of infected plant material. The first infected plant material was from diseased plants in the field (*in vivo*). This material showed three levels of symptoms: (a) witches' broom leaves, (b) phyllody leaves and (c) apparently normal leaves (but from diseased plants). The other infected plant material was from sterile (*in vitro*) cultured tissues of JWB plantlets. The phytoplasma concentrations in the *in vivo* material with three levels of symptoms were measured by Xue *et al.* (2018) [22]. The phytoplasma determination in the *in vitro* tissues shows fluorescent spots forming a large circle in the

phloem of the petiole (**Additional file 5**). These results confirm the subsequent tests on *ZjMAPKKK* function in response to phytoplasma infection.

Expression analysis of *ZjMAPKKKs* in witches' broom leaves

In **Additional file 9** and **Fig. 6 (A)**, the heat map shows the expression levels of *ZjMAPKKKs* with significantly different patterns in the witches' broom leaves from June to September. There were 42 candidates expressing at a detectable level, but the expression levels of the other 14 *ZjMAPKKKs* were either not expressed or were expressed at levels below our detection threshold. The *ZjMAPKKKs* genes with too low (or nonexistent) expression were rejected as candidates for further calculation and analysis. Among these genes, the most significant transcript induction took place in the early stage (June or July) when the concentration of witches' broom began to increase. For example, *ZjMAPKKK13, -14, -15, -23, -34, -42, -44, -47* and *-56* were significantly induced in June or July, but induction later decreased from August to September, as shown in **Fig. 6 (B)**. However, *ZjMAPKKK3, -43* and *-50* were downregulated from June to September. The expression levels of two *ZjMAPKKK* members (*ZjMAPKKK26* and *-45*) remained high from June to September. This finding may indicate that these are key *MAPKKKs* in response to phytoplasma infection. However, the clustering of *ZjMAPKKK* expression profiles was not aligned with gene similarities, illustrating that gene function may not rely on gene structure.

Expression analysis of *ZjMAPKKKs* in phyllody leaves

The transcript abundance of *ZjMAPKKKs* was also investigated in phyllody leaves. The heat map of the expressing *ZjMAPKKKs* is shown in **Fig. 7 (A)**. Several of the *ZjMAPKKKs* were highly expressed in June or July, but their expression levels then decreased from August to September. However, most *ZjMAPKKKs* showed no significant changes in expression level. Expression details for all *ZjMAPKKKs* are shown in **Fig. 7 (B)**. *ZjMAPKKK10, -14, -15 -34, -44* and *-56* were all significantly upregulated in the early stage (June or July). However, ten of the *ZjMAPKKKs* (*ZjMAPKKK3, -16, -18, -41, -43, -50, -51, -52, -53* and *-55*) were significantly downregulated. As in the witches' broom leaves, in the phyllody leaves, *ZjMAPKKK26* and *-45* were highly upregulated from June to September.

Expression analysis of *ZjMAPKKKs* in apparently normal leaves

The apparently normal but asymptomatic infected leaves were used to test which *ZjMAPKKKs* play a role in the phytoplasma infection response. Interestingly, the heat map figure shows different expression patterns for *ZjMAPKKKs* in these leaves (**Fig. 8B**). A few genes were highly upregulated, but most showed downregulation. For example, *ZjMAPKKK1, -3, -7, -16, -17, -18, -19, -41, -43, -50,* and *-52* were downregulated from June to September, while *ZjMAPKKK28, -34* and *-47* were significantly upregulated in June or July, while *ZjMAPKKK*27 and -54 were upregulated from August or September. However, *ZjMAPKKK*26 and -45 showed the same pattern of high expression in the asymptomatic infected leaves from June to September (**Fig. 8 A**).

To summarise, in the phytoplasma-infected tissues of the three symptomatic severities (apparently normal, phyllody and witches' broom) and in the four months (June through September), *ZjMAPKKK26* was significantly upregulated, and *ZjMAPKKK45* was also highly induced. As the infection developed, the visible disease symptoms increased, becoming gradually more severe, from apparently normal leaves to phyllody

leaves to witches' broom leaves [21]. This progression occurred even though the concentration of JWB decreased gradually from August through September. The expression of *ZjMAPKKK26* increased approximately six-fold in the phyllody leaves in June but not at the other two symptomatic levels. Then, as the infection developed, *ZjMAPKKK26* was upregulated approximately three-fold in the witches' broom leaves in July but downregulated in the phyllody. Meanwhile, in June, the induction of *ZjMAPKKK45* increased approximately three-fold in the apparently normal (but phytoplasma-infected) leaves and approximately six-fold in the phyllody leaves. Then, during July, August and September, it was downregulated, but induction in the witches' broom leaves remained approximately constant (**Fig. 6, 7 and 8**). These results show that *ZjMAPKKK26* responds quickly in phyllody leaves and is highly induced in witch broom leaves, while *ZjMAPKKK45* responds more rapidly than *ZjMAPKKK26,* as indicated by its high expression in apparently normal leaves in June. In contrast to *ZjMAPKKK26* and *ZjMAPKKK45,* which were significantly upregulated, *ZjMAPKKK3, ZjMAPKKK43* and *ZjMAPKKK50* were significantly downregulated.

Expression analysis of the *ZjMAPKKKs* in sterile cultured JWB plantlets

In addition to the *ZjMAPKKK* expression profiles in the *in vivo* field tissues, we also examined expression levels in the *in vitro* cultured JWB plantlets, with uninfected plantlets being used as a control. As shown in **Fig. 9**, the *in vitro ZjMAPKKK* expression profiles differed significantly from the *in vivo* profiles. Only four of the *ZjMAPKKKs* were significantly induced in the diseased plants - *ZjMAPKKK4, -10, -25* and *-44*. *ZjMAPKKK6, -7, -17, -18, -30, -34, -35, -37, -40, -41, -43, -46, -52* and *-53* were significantly downregulated. The other *ZjMAPKKKs* showed no significant change.

Discussion

The *MAPK* cascades are highly conserved, signal-transducing modules found in eukaryotes. These cascades have been widely studied in the plant kingdom, including in *Arabidopsis*, rice, maize, and apple [6, 10, 13, 14, 16]. Ten *MAPKs* and five *MAPKKs* have already been identified in Chinese jujube [18]. The structures of these genes were mostly shown to be similar to those found in other plants (e.g., *Arabidopsis*, poplar, and apple [18]). In this study, for the first time, we report on *MAPKKKs* in the Chinese jujube genome. We identified 56 *ZjMAPKKKs* in Chinese jujube. This number is somewhat larger than that of *VviMAPKKKs* in grapevine [15] but smaller than that of *MdMAPKKKs* in apple [16]. The *ZjMAPKKKs* can be classified into the two main subfamilies Raf and MEKK, with none belonging to the subfamily ZIK. The disappearance of the ZIK subfamily may be due to a loss of function during the evolution of Chinese jujube because the Raf subfamily is considered to be the origin of the *MAPKKK* family [33]. In addition, the rate of intron loss is known to be more rapid than that of intron gain due to segmental duplication [34]. In this study, we found that the number of conserved motifs and exons was higher in the Raf subfamily than in the MEKK subfamily. We also identified 13 segmental duplication events among 22 *ZjMAPKKKs*. This finding may indicate that the Raf subfamily contains original genes and that segmental duplication occurred during a long evolutionary history. This interpretation is consistent with that for maize [14]. Furthermore, 43 of the *ZjMAPKKKs* were widely located over the 12 chromosomes, while chromosome positions could not be found for *ZjMAPKKK44-56* (**Table 1**). These findings indicate that evolutionary duplications of *ZjMAPKKKs* took place and that the unknown locations of many *ZjMAPKKKs* may confer a number of paralogous genes and play critical roles in

various biological processes. For example, *ZjMAPKKK44, -45, -46,* and *-50* may be involved in processes associated with phytoplasma infection. This result is different from that obtained in our previous study on *ZjMAPKs* and *ZjMAPKKs*, which did not show genome duplication in the evolutionary process [18].

MAPK cascades have been shown to be key signalling modules operating in response to biotic and abiotic stresses, particularly associated with pathogen attack [35]. Among the *MAPKKKs*, the MEKK subfamily has been widely studied, while the biological functions of the Raf subfamily are still somewhat obscure. In *Arabidopsis*, the MAPK cascade signalling module *MEKK1-MKK4/MKK5-MPK3/MPK6* is proposed to be activated in the interaction with *flg22* treatment [36]. *EDR1*, a member of the Raf subfamily, is responsible for salicylic acid-induced powdery mildew attack [37]. In tomato, *MAPKKKε* and *MAPKKKα* play important roles in cell death signalling associated with plant immunity [38, 39]. In wheat, a *MAPKKK* named *TaFLR* can be activated by the leaf rust pathogen *Puccinia triticina* [40]. In grapevine, *VqMAPKKK38* can be highly induced by powdery mildew infection [41]. All the evidence suggests that members of MAPKKKs are essential in pathogen attack signal transduction. In this study, we demonstrate that *ZjMAPKKK26* and *-45* are significantly upregulated and *ZjMAPKKK3, -43* and *-50* are downregulated in the three main symptomatic phases of witches' broom disease at different time stages. Meanwhile, in the *in vitro* culture of JWB, four *ZjMAPKKKs* (*ZjMAPKKK4, -10, -25* and *-44*) were significantly induced in the diseased plants, while fourteen *ZjMAPKKKs* (*ZjMAPKKK6, -7, -17, -18, -30, -34, -35, -37, -40, -41, -43, -46, -52* and *-53*) were significantly downregulated. The potential candidate gene responses to phytoplasma were different *in vivo* and *in vitro.* This result is consistent with the findings of our previous work in which we found that *ZjMPK1* was the gene potentially related to phytoplasma infection *in vitro* [18] but was different from our later finding that *ZjMPK2* was likely regulating along with *ZjMEK2in vivo* [24]. The reason behind this phenomenon may be that many more environmental factors (e.g., light and temperature) affect the development of a phytoplasma infection *in vivo*. Even so, all the candidates discussed above could be involved in phytoplasma infection signal transduction by recruiting the *MAPKK* and *MAPK* families. Moreover, *ZjMAPKKK43* (homologous to *AtRaf1* in *Arabidopsis*) was downregulated in all the infected tissues, while *ZjMAPKKK10* was highly induced in the *in vivo* JWB plantlets. This gene is homologous to *AtMEKK1* in *Arabidopsis*. Thus, these two genes may both be key to the response to phytoplasma infection in Chinese jujube because *AtMEKK1* has already been shown to be important in innate immunity in *Arabidopsis* by activating *MKK4/MKK5-MPK3/MPK6* [36]. Moreover, *ZjMKK2* could activate *ZjMPK2* and thus play essential roles in the JWB defence response [24]. Ye *et al.* [23] have shown that after phytoplasma infection, MAPKs can also be activated and that the transcription factor *WRKY33* is regulated. Taken together, these results indicate the likely *ZjMAPKKKs* that mediate *ZjMKK2-ZjMPK2* to *WRKY* transcription factors in response to phytoplasma infection, which will need to be resolved in future studies. In addition, the scaffold *RACK 1* (Receptor for Activated C Kinase 1) has been identified in *Arabidopsis,* which tethers *MAPKKKs* to the plasma membrane and associates with the Gb subunit involved in immune responses [42]. Therefore, in future studies, it may be worth investigating the functions of these *MAPKKK* candidates and their relationships to *RACK1* in response to phytoplasma infection of Chinese jujube.

Conclusions

Using a range of informatics analyses of *MAPKKKs* in the Chinese jujube genome, 56 members were identified and named *ZjMAPKKK* according to their locations on the chromosomes. The phylogeny, conserved motifs and intron/exon analyses confirm the identity of these kinases as members of each subfamily. The expression profiles of the *ZjMAPKKKs* were recorded by qPCR in materials at four timings and exhibiting three levels of JWB symptoms (witches' broom leaves, phyllody leaves and apparently normal leaves) and in sterile *in vitro* cultures of JWB plantlets. *ZjMAPKKK26* and *-45* were significantly upregulated and *ZjMAPKKK3, -43* and *-50* were downregulated in the three main infected tissues. Meanwhile, in the sterile cultivated tissues of JWB plantlets, four *ZjMAPKKKs* (*4, 10, 25* and *-44*) were significantly induced in the diseased plants. Additionally, *ZjMAPKKK6, -7, -17, -18, -30, -34, -35, -37, -40, -41, -43, -46, -52* and *-53* were significantly downregulated. Our results provide early insight into certain *ZjMAPKKKs* that could be involved in the plant response to phytoplasma infection.

Declarations

Ethics approval and consent to participate

The healthy and diseased jujube trees used in this study were from the Experimental Station of Chinese Jujube, Hebei Agricultural University, in Baoding, Hebei. Chinese jujube is one of traditional and widespread fruit trees in China, and it is not an endangered species. No specific permits are required for sample collection on Chinese jujube.

Consent for publication

Not applicable.

Ethical standards

This research does not contain any studies with human participants or animals.

Availability of data and materials

All data and materials are presented in the main paper and additional file. In addition, the whole protein sequences of MAPKKKs in *Arabidopsis* were retrieved from TAIR databases. The CDS and genome sequences of MAPKKKs in jujube were retrieved from the whole jujube genome database (accession JREP00000000) in NCBI.

Competing interests

The authors declare that they have no competing interests.

Funding

This work was supported by the Funds for Hebei Distinguished Young Scholar (C2016204145), the Youth Fund of Hebei Province Natural Science Foundation (C2016204157), Green Channel Fund of Hebei Province Natural Science Foundation (C2019204308), the Significance Fund of Hebei Province Natural Science

Foundation (C2017204114), and the Agricultural University of Hebei Foundation for Leaders of Disciplines in Science Technology, Funds for Young Talent Project of Hebei Agricultural University Foundation (grant number YJ201853). Funds were used for the design of the study and collection, analysis, and interpretation of data and in writing the manuscript, as well as in the open access payment.

Authors' contributions

JZ and ML designed the research and wrote the paper. ZL and LW performed the experiments, analyzed the data and wrote the paper. CX, YC, WG and YZ performed the experiments and participated in the data analysis. All authors read and approved the final the manuscript.

Acknowledgement

Not applicable.

Abbreviations

JWB: Jujube witches' broom; **S-TKc:** Serine/threonine protein kinase; **MAPK:** Mitogen-activated protein kinase; **MAPKK:** MAPK kinase; **MAPKKK:** MAPK kinase kinase; **ORF:** Open reading frames; **qPCR:** Quantitative real-time PCR; ***Zj*:** *Ziziphus jujuba*□**Chr:** Chromosome; **PI:** The theoretical isoelectric point of proteins; **MW:** The theoretical molecular weight of proteins; **RACK 1:** Receptor for Activated C Kinase 1

References

1. Rodriguez MCS, Petersen M, Mundy J. Mitogen-Activated Protein Kinase Signaling in Plants. Annu Rev Plant Biol. 2010; 61:621-649.
2. Sinha AK, Jaggi M, Raghuram B, Tuteja N. Mitogen-activated protein kinase signaling in plants under abiotic stress. Plant signaling & behavior. 2011; 6(2):196-203.
3. Galletti R, Ferrari S, De Lorenzo G. Arabidopsis MPK3 and MPK6 Play Different Roles in Basal and Oligogalacturonide- or Flagellin-Induced Resistance against Botrytis cinerea. Plant Physiol. 2011; 157(2):804-814.
4. Jonak C, Okresz L, Bogre L, Hirt H. Complexity, cross talk and integration of plant MAP kinase signalling. Curr opin plant biol. 2002; 5(5):415-424.
5. Rodriguez MC, Petersen M, Mundy J. Mitogen-activated protein kinase signaling in plants. Annu Rev Plant Biol. 2010; 61:621-649.
6. Group M. Mitogen-activated protein kinase cascades in plants: a new nomenclature. Trends Plant Sci. 2002; 7(7):301-308.
7. Zhang S, Klessig DF. MAPK cascades in plant defense signaling. Trends Plant Sci. 2001; 6(11):520-527.
8. Asai T, Tena G, Plotnikova J, Willmann MR, Chiu WL, Gomez-Gomez L, Boller T, Ausubel FM, Sheen J. MAP kinase signalling cascade in Arabidopsis innate immunity. Nature. 2002; 415(6875):977-983.
9. Pitzschke A, Djamei A, Bitton F, Hirt H. A major role of the MEKK1-MKK1/2-MPK4 pathway in ROS signalling. Molecular plant. 2009; 2(1):120-137.

10. Kong Q, Qu N, Gao MH, Zhang ZB, Ding XJ, Yang F, Li YZ, Dong OX, Chen S, Li X. The MEKK1-MKK1/MKK2-MPK4 Kinase Cascade Negatively Regulates Immunity Mediated by a Mitogen-Activated Protein Kinase Kinase Kinase in Arabidopsis. Plant Cell. 2012; 24(5):2225-2236.
11. Liu Y, Schiff M, Dinesh-Kumar SP. Involvement of MEK1 MAPKK, NTF6 MAPK, WRKY/MYB transcription factors, COI1 and CTR1 in N-mediated resistance to tobacco mosaic virus. The Plant J. 2004; 38(5):800-809.
12. Ekengren SK, Liu Y, Schiff M, Dinesh-Kumar SP, Martin GB. Two MAPK cascades, NPR1, and TGA transcription factors play a role in Pto-mediated disease resistance in tomato. The Plant J. 2003; 36(6):905-917.
13. Rao KP, Richa T, Kumar K, Raghuram B, Sinha AK. In silico analysis reveals 75 members of mitogen-activated protein kinase kinase kinase gene family in rice. DNA Res. 2010; 17(3):139-153.
14. Liu Y, Zhou M, Gao Z, Ren W, Yang F, He H, Zhao J. RNA-Seq Analysis Reveals MAPKKK Family Members Related to Drought Tolerance in Maize. Plos One. 2015; 10(11):e0143128.
15. Wang G, Lovato A, Polverari A, Wang M, Liang YH, Ma YC, Cheng ZM. Genome-wide identification and analysis of mitogen activated protein kinase kinase kinase gene family in grapevine (Vitis vinifera). BMC plant biol. 2014; 14:219.
16. Sun M, Xu Y, Huang J, Jiang Z, Shu H, Wang H, Zhang S. Global Identification, Classification, and Expression Analysis of MAPKKK genes: Functional Characterization of MdRaf5 Reveals Evolution and Drought-Responsive Profile in Apple. Sci Rep. 2017; 7(1):13511.
17. Wang L, Hu W, Tie W, Ding Z, Ding X, Liu Y, Yan Y, Wu C, Peng M, Xu B. The MAPKKK and MAPKK gene families in banana: identification, phylogeny and expression during development, ripening and abiotic stress. Sci Rep. 2017; 7(1):1159.
18. Liu ZG, Zhang LM, Xue CL, Fang H, Zhao J, Liu MJ. Genome-wide identification and analysis of MAPK and MAPKK gene family in Chinese jujube (*Ziziphus jujuba* Mill.). BMC Genomics. 2017; 18.
19. Jung HY, Sawayanagi T, Kakizawa S, Nishigawa H, Wei W, Oshima K, Miyata S, Ugaki M, Hibi T, Namba S. 'Candidatus Phytoplasma ziziphi', a novel phytoplasma taxon associated with jujube witches'-broom disease. Int J Syst Evol Micr. 2003; 53:1037-1041.
20. Liu MJ, Zhao J, Zhou JY. Jujube Witches' Broom Disease. China Agriculture Press, Beijing, 2010 (In Chinese).
21. Lee S, Kim CE, Cha B. Migration and Distribution of Graft-inoculated Jujube Witches'-broom Phytoplasma within a Cantharanthus roseus Plant. Plant Pathology J. 2012; 28(2):191-196.
22. Xue C, Liu Z, Dai L, Bu J, Liu M, Zhao Z, Jiang Z, Gao W, Zhao J. Changing Host Photosynthetic, Carbohydrate, and Energy Metabolisms Play Important Roles in Phytoplasma Infection. Phytopathology. 2018; 108(9):1067-1077.
23. Ye X, Wang HY, Chen P, Fu B, Zhang MY, Li JD, Zheng XB, Tan B, Feng JC. Combination of iTRAQ proteomics and RNA-seq transcriptomics reveals multiple levels of regulation in phytoplasma-infected Ziziphus jujuba Mill. Hortic Res-England. 2017; 4.
24. Liu ZG, Zhao Z, Xue CL, Wang LL, Wang LL, Feng C, Liu MJ. Three Main Genes in the MAPK Cascade Involved in the Chinese Jujube-Phytoplasma Interaction. Forests. 2019; 10(5):392.

25. Liu MJ, Zhao J, Cai QL, Liu GC, Wang JR, Zhao ZH, Liu P, Dai L, Yan GJ, Wang WJ. The complex jujube genome provides insights into fruit tree biology. Nat Commun. 2014; 5.
26. Wang J, Pan CT, Wang Y, Ye L, Wu J, Chen LF, Zou T, Lu G. Genome-wide identification of MAPK, MAPKK, and MAPKKK gene families and transcriptional profiling analysis during development and stress response in cucumber. BMC Genomics. 2015; 16.
27. Gasteiger E, Gattiker A, Hoogland C, Ivanyi I, Appel RD, Bairoch A. Expasy: the proteomics server for in-depth protein knowledge and analysis. Nucleic acids res. 2003; 31(13):3784-3788.
28. Guo AY, Zhu QH, Chen X, Luo JC. [GSDS: a gene structure display server]. Yi chuan = Hereditas. 2007; 29(8):1023-1026.
29. Bailey TL, Elkan C. Fitting a mixture model by expectation maximization to discover motifs in biopolymers. Proceedings International Conference on Intelligent Systems for Molecular Biology. 1994; 2:28-36.
30. Neupane A, Nepal MP, Piya S, Subramanian S, Rohila JS, Reese RN, Benson BV. Identification, nomenclature, and evolutionary relationships of mitogen-activated protein kinase (MAPK) genes in soybean. Evolutionary bioinformatics online. 2013; 9:363-386.
31. Livak KJ, Schmittgen TD. Analysis of relative gene expression data using real-time quantitative PCR and the 2(T)(-Delta Delta C) method. Methods. 2001; 25(4):402-408.
32. Bu J, Zhao J, Liu M. Expression Stabilities of Candidate Reference Genes for RT-qPCR in Chinese Jujube (*Ziziphus jujuba* Mill.) under a Variety of Conditions. Plos One. 2016; 11(4):e0154212.
33. Ye JQ, Yang H, Shi HT, Wei YX, Tie WW, Ding ZH, Yan Y, Luo Y, Xia ZQ, Wang WQ. The MAPKKK gene family in cassava: Genome-wide identification and expression analysis against drought stress. Sci Rep. 2017; 7.
34. Nuruzzaman M, Manimekalai R, Sharoni AM, Satoh K, Kondoh H, Ooka H, Kikuchi S. Genome-wide analysis of NAC transcription factor family in rice. Gene. 2010; 465(1-2):30-44.
35. Pitzschke A, Schikora A, Hirt H. MAPK cascade signalling networks in plant defence. Curr opin plant biol. 2009; 12(4):421-426.
36. Colcombet J, Hirt H. *Arabidopsis* MAPKs: a complex signalling network involved in multiple biological processes. Biochem J. 2008; 413:217-226.
37. Wu GH, Liu SM, Zhao YF, Wang W, Kong ZS, Tang DZ. ENHANCED DISEASE RESISTANCE4 Associates with CLATHRIN HEAVY CHAIN2 and Modulates Plant Immunity by Regulating Relocation of EDR1 in *Arabidopsis*. Plant Cell. 2015; 27(3):857-873.
38. del Pozo O, Pedley KF, Martin GB. MAPKKK alpha is a positive regulator of cell death associated with both plant immunity and disease. Embo J. 2004; 23(15):3072-3082.
39. Melech-Bonfil S, Sessa G. Tomato MAPKKK epsilon is a positive regulator of cell-death signaling networks associated with plant immunity. Plant Journal. 2010; 64(3):379-391.
40. Gao Y, Stebbing J, Tubei K, Tian LN, Li XQ, Xing T. Response of TaFLR MAPKKK to wheat leaf rust and Fusarium head blight and the activation of downstream components. Trop Plant Pathol. 2016; 41(1):15-23.

41. Jiao YT, Wang D, Wang L, Jiang CY, Wang YJ. VqMAPKKK38 is essential for stilbene accumulation in grapevine. Hortic Res-England. 2017; 4.
42. Su JB, Xu J, Zhang SQ. RACK1, scaffolding a heterotrimeric G protein and a MAPK cascade. Trends Plant Sci. 2015; 20(7):405-407.

Tables

Table 1 Characteristic of MAPK Kinase Kinases from *Ziziphus Jujuba* Mill. (*ZjMAPKKKs*)

Group	Name	Locus ID	Chr	Location	CDS (bp)	Amino acid length (AA)	PI	MW (KD)
Raf	ZjMAPKKK1	LOC107412947	Chr1	512097-518184	3351	1116	5.56	123.87
	ZjMAPKKK2	LOC101223021	Chr1	588730..592155	1062	353	7.16	39.83
	ZjMAPKKK3	LOC107413171	Chr1	6034745..6041047	1380	459	8.99	52.10
	ZjMAPKKK4	LOC107414729	Chr1	7211380..7216386	1119	372	9.01	42.35
	ZjMAPKKK5	LOC107422643	Chr1	17322629..17330021	1707	568	6.55	64.31
	ZjMAPKKK7	LOC107427772	Chr1	28684428..28693993	4455	1484	5.27	160.66
	ZjMAPKKK8	LOC107429777	Chr1	31236415..31242279	3432	1143	7.67	126.67
	ZjMAPKKK11	LOC107412267	Chr2	23790620..23798118	2913	970	5.83	107.05
	ZjMAPKKK13	LOC107415263	Chr4	1873602..1877368	1059	352	7.66	39.46
	ZjMAPKKK14	LOC107417160	Chr4	23620629..23633413	2208	735	6.1	83.02
	ZjMAPKKK15	LOC107417666	Chr5	2301847..2306994	1248	415	8.14	46.31
	ZjMAPKKK16	LOC107417677	Chr5	2314642..2318435	1257	418	7.62	46.80
	ZjMAPKKK17	LOC107417907	Chr5	5814146..5820584	3789	1262	5.18	139.68
	ZjMAPKKK18	LOC107417903	Chr5	5822068..5828809	3825	1274	5.43	140.42
	ZjMAPKKK19	LOC107418405	Chr5	10268020..10272429	1074	357	8.97	40.45
	ZjMAPKKK20	LOC107418996	Chr5	18139031..18145136	2343	780	6.38	87.04
	ZjMAPKKK22	LOC107421353	Chr6	17987031..17997512	2832	943	8.15	105.39
	ZjMAPKKK23	LOC107420099	Chr6	2889952..2898479	2856	951	5.53	104.94
	ZjMAPKKK24	LOC107422567	Chr7	14102760..14109942	3444	1147	5.87	127.99
	ZjMAPKKK26	LOC107423093	Chr7	21216345..21219607	1173	390	7.92	43.53
	ZjMAPKKK27	LOC107423594	Chr7	27636786..27641226	1251	416	6.11	46.81
	ZjMAPKKK28	LOC107424157	Chr8	4344698..4348053	2049	682	8.81	79.10
	ZjMAPKKK30	LOC107424832	Chr8	9154812..9160628	1179	392	9.11	44.23
	ZjMAPKKK32	LOC107426395	Chr9	4943575..4946720	1203	400	6.29	44.66
	ZjMAPKKK33	LOC107426719	Chr9	5733599..5742140	3945	1314	5.32	144.52
	ZjMAPKKK34	LOC107427400	Chr9	18534579..18538786	1032	343	5.84	38.71
	ZjMAPKKK38	LOC107428906	Chr10	10418263..10423580	1299	432	8.15	48.84
	ZjMAPKKK39	LOC107428931	Chr10	11520310..11525561	1299	432	7.74	48.89
	ZjMAPKKK41	LOC107430036	Chr11	2650983..2657196	2181	726	6.97	81.01
	ZjMAPKKK42	LOC107431473	Chr11	19821853..19829329	1707	568	5.51	64.02
	ZjMAPKKK43	LOC107432147	Chr12	5159272..5168476	2556	851	5.98	93.67
	ZjMAPKKK45	LOC107408109	Unplaced Scaffold	688..6689	1425	474	9.12	53.23
	ZjMAPKKK46	LOC107405634	Unplaced Scaffold	5820..12905	1341	446	5.58	50.42
	ZjMAPKKK47	LOC107407393	Unplaced Scaffold	6471..11148	1125	374	7.13	42.29
	ZjMAPKKK48	LOC107406964	Unplaced Scaffold	13195..15977	1005	334	7.68	37.91
	ZjMAPKKK49	LOC107404883	Unplaced Scaffold	14404..17983	1251	416	6.24	46.77
	ZjMAPKKK50	LOC107406505	Unplaced Scaffold	16102..20361	1059	352	7.17	39.84
	ZjMAPKKK51	LOC107405705	Unplaced Scaffold	33936..39585	1158	385	7.51	42.93
	ZjMAPKKK52	LOC107403422	Unplaced Scaffold	48143..64604	1647	548	5.13	61.65
	ZjMAPKKK53	LOC107435406	Unplaced Scaffold	61008..63977	1479	492	9.34	56.56
	ZjMAPKKK55	LOC107435407	Unplaced Scaffold	134848..138183	1482	493	9.22	56.35
MEKK	ZjMAPKKK6	LOC107423632	Chr1	18688160..18695042	2700	899	9.29	96.87

ZjMAPKKK9	LOC107432528	Chr1	34451996..34453515	1428	475	4.78	53.09
ZjMAPKKK10	LOC107411974	Chr2	21809712..21815908	2046	681	5.64	74.86
ZjMAPKKK12	LOC107414154	Chr3	19912625..19913971	1266	421	4.95	46.85
ZjMAPKKK21	LOC107420999	Chr6	10913503..10919747	1839	612	5.53	67.87
ZjMAPKKK25	LOC107423026	Chr7	20770505..20775489	2058	685	6.78	75.80
ZjMAPKKK29	LOC107424505	Chr8	6765530..6767083	1071	356	4.93	39.97
ZjMAPKKK31	LOC107425633	Chr8	20944047..20949800	1563	520	9.11	56.65
ZjMAPKKK35	LOC107427543	Chr9	20198543..20199481	939	312	6.52	35.52
ZjMAPKKK36	LOC107428154	Chr10	1469136..1470695	762	253	7.01	28.29
ZjMAPKKK37	LOC107428813	Chr10	8441149..8442948	825	274	4.89	30.43
ZjMAPKKK40	LOC107429056	Chr10	13522021..13523553	1035	344	5.36	37.67
ZjMAPKKK44	LOC107409320	Unplaced Scaffold	335..2009	1335	444	4.8	50.18
ZjMAPKKK54	LOC107434197	Unplaced Scaffold	108777..110183	1119	372	5.46	41.39
ZjMAPKKK56	LOC107435014	Unplaced Scaffold	155489..160603	1836	611	5.64	67.84

Note: Chr: chromosome; PI: the theoretical isoelectric point of proteins; MW: The theoretical molecular weight of proteins.

Additional Files

Additional file 1: Fig. S1 Protein sequences of MAPKKKs from *Ziziphus jujuba* Mill. and *Arabidopsis thaliana*.

Additional file 2: Table S1 Number of main protein domains of ZjMAPKKKs.

Additional file 3: Fig. S2 Healthy and diseased *in vitro* plantlets. A: Healthy plantlets; B: Diseased plantlets.

Additional file 4: Fig. S3 Tissues showing different JWB disease symptoms. A: Witches' broom leaves; B: Phyllody leaves; C: Apparently normal leaves; D: Healthy leaves. A, B and C were used as a test group collected from diseased trees. D was used as a control collected from healthy trees.

Additional file 5: Fig. S4: Determination of phytoplasma in the sieve element in jujube petiole phloem by using 4',6-diamidino-2-phenylindole (DAPI). A, No fluorescent spots were observed in the sieve element (SE) of healthy plantlets. B, The fluorescent spots formed a large, bright circle in the sieve element (SE) of the diseased plantlets. The numbers and sizes of the fluorescent spots indicate the number of phytoplasmas. Bar = 100 μm.

Additional file 6: Table S2 Primer sequences of *ZjMAPKKKs* for qRT-PCR.

Additional file 7: Fig. S5 CDS sequences of *ZjMAPKKKs.*

Additional file 8: Table S3 Number of introns and exons of *ZjMAPKKK* genes

Additional file 9: Table S4 Fold-change values of *ZjMAPKKKs* in the leaves of witches' broom, phyllody and apparently normal symptoms.

Figures

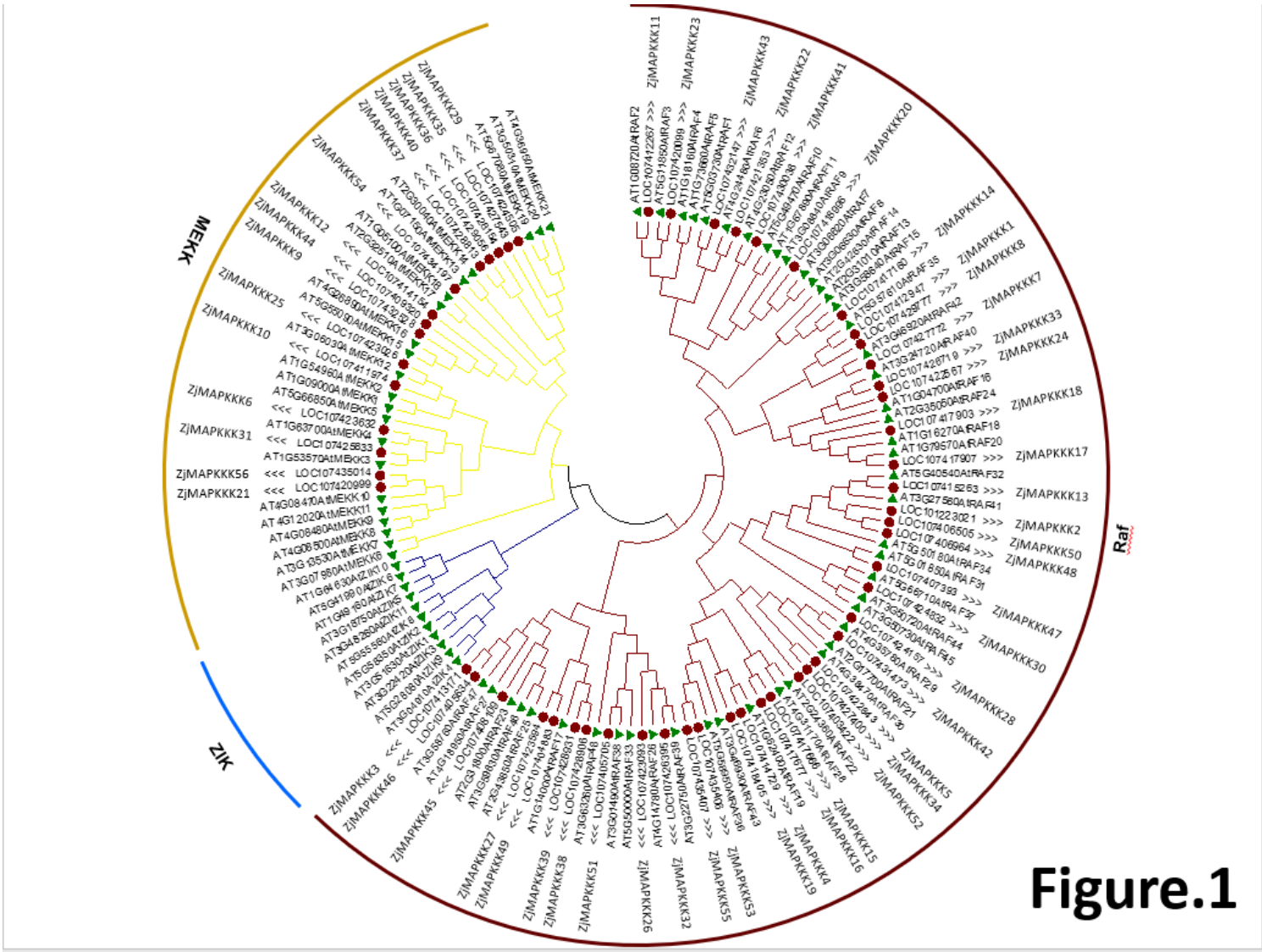

Figure 1

Phylogenetic analyses of ZjMAPKKKs (Ziziphus jujuba Mill.) and AtMAPKKKs (Arabidopsis thaliana) with a total of 136 protein sequences. MEGA 6.0 was used to construct the phylogenetic tree employing the neighbour-joining (NJ) method. A total of 1,000 bootstrap replications were carried out to indicate reliability. The ZjMAPKKKs were clustered into two groups - the Raf and MEKK subfamilies.

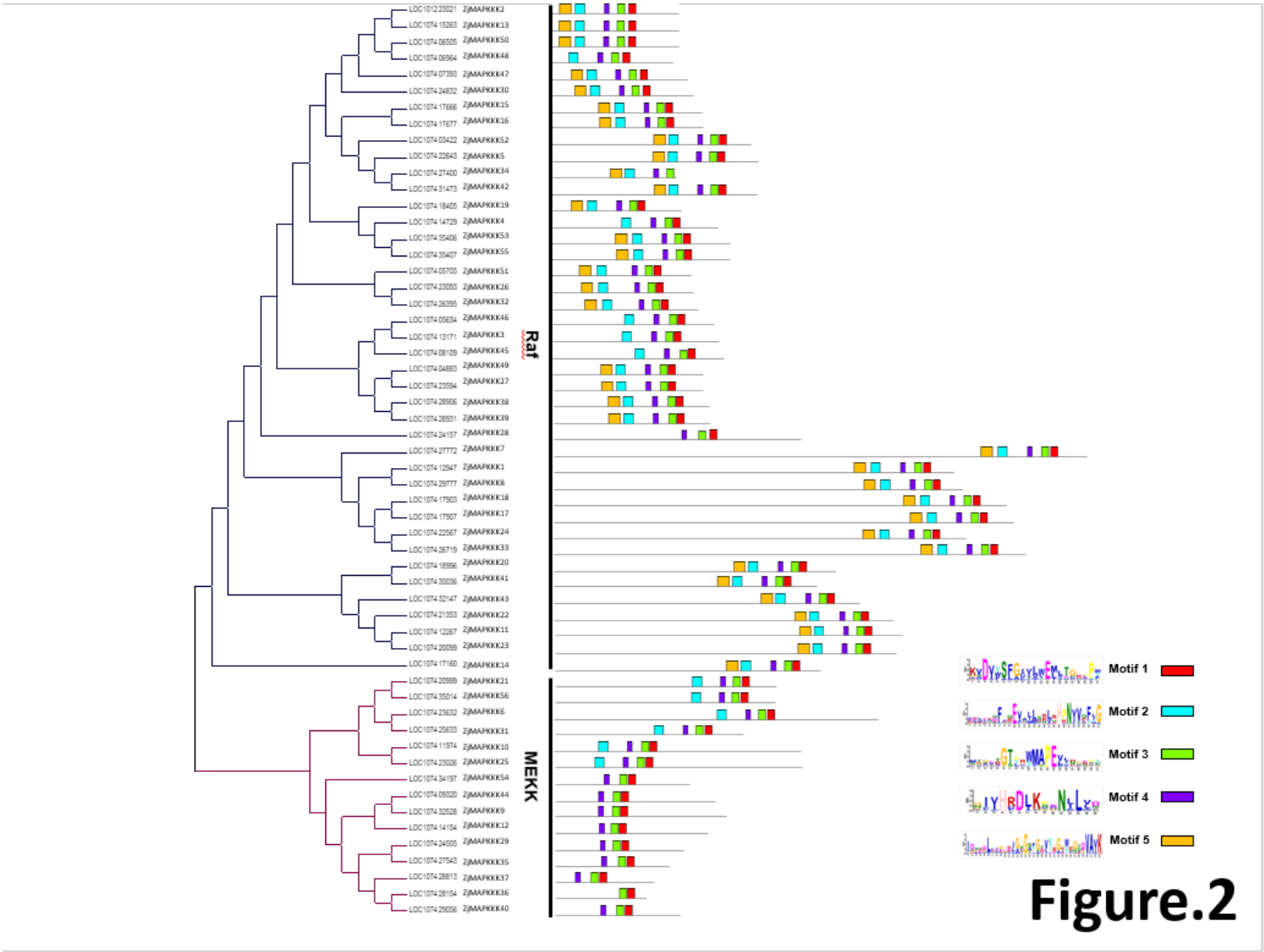

Figure 2

Identification of the conserved motifs of ZjMAPKKKs corresponding to the phylogenetic tree. The MEME database was used to identify the motifs based on protein sequences.

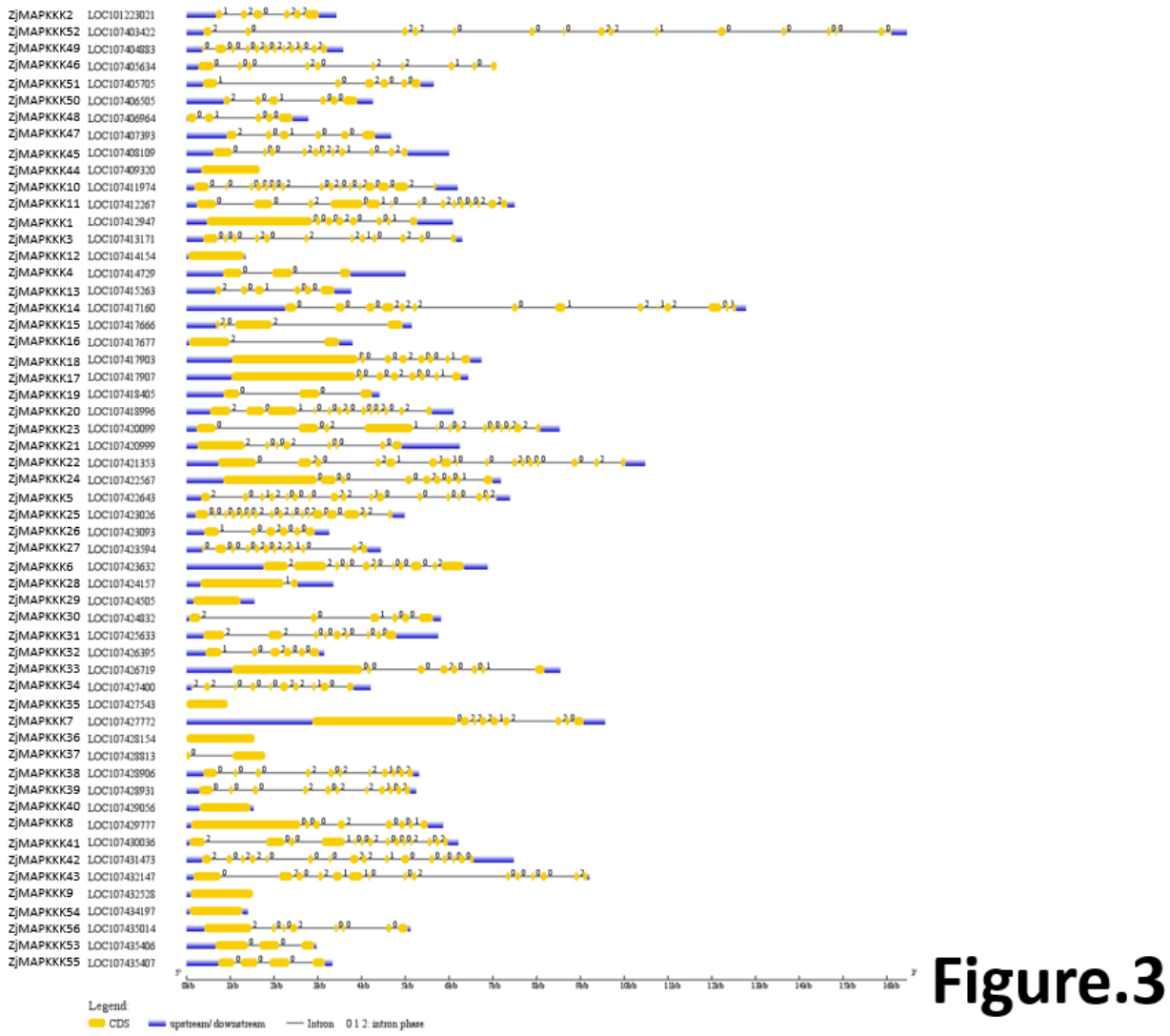

Figure.3

Figure 3

Schematic diagrams of ZjMAPKKK structures. The yellow and blue boxes and the black lines indicate exons, UTRs and introns, respectively. The numerals 0, 1 and 2 indicate different intron phases.

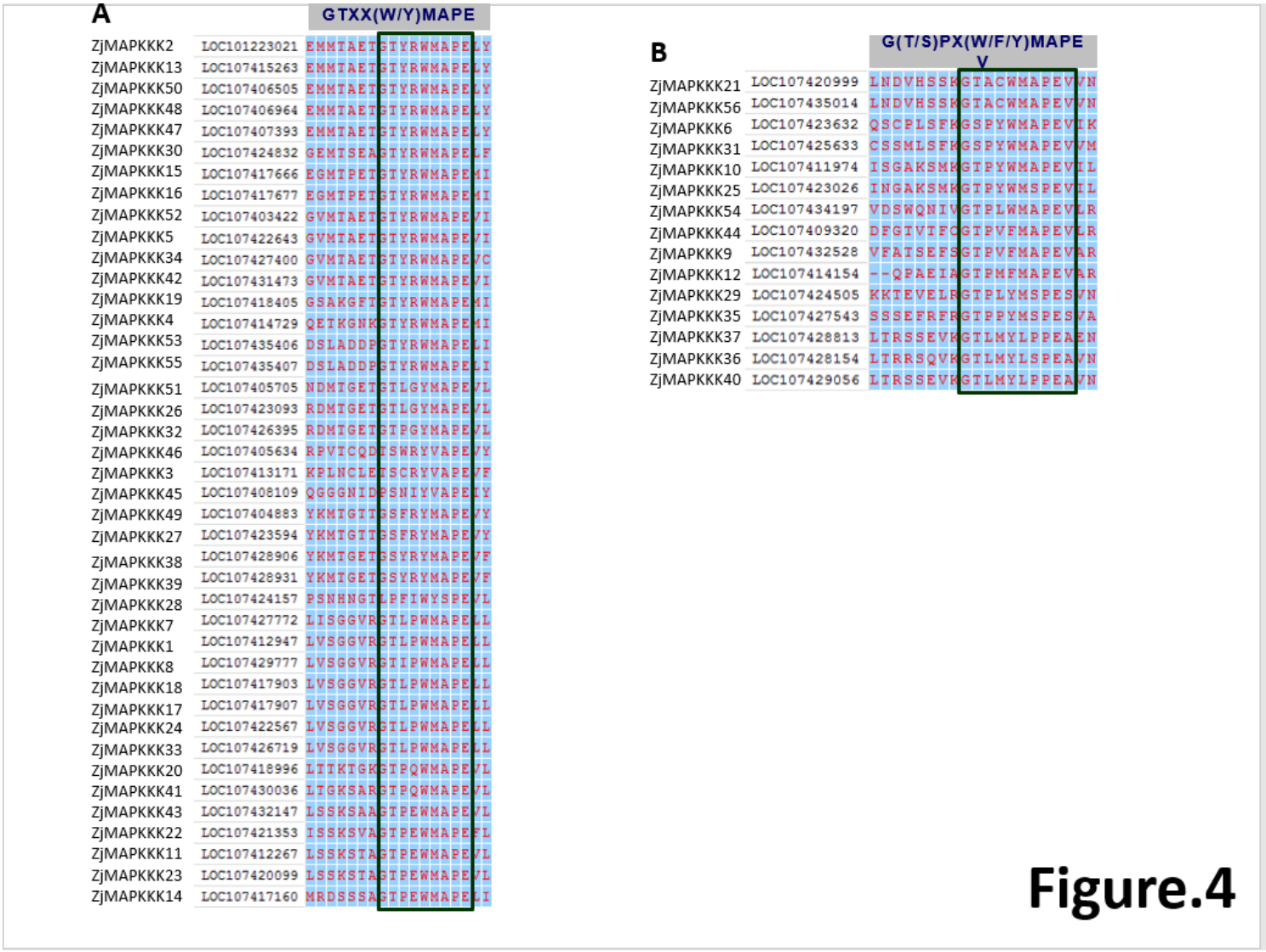

Figure 4

Protein sequence alignment of the Raf subfamily (A) and MEKK subfamily (B) from Ziziphus jujuba Mill. The conserved signature motifs GTXX(W/Y)MAPE and GTPEFMAPE(L/V)(Y/F) were found in the Raf and MEKK subfamilies, respectively.

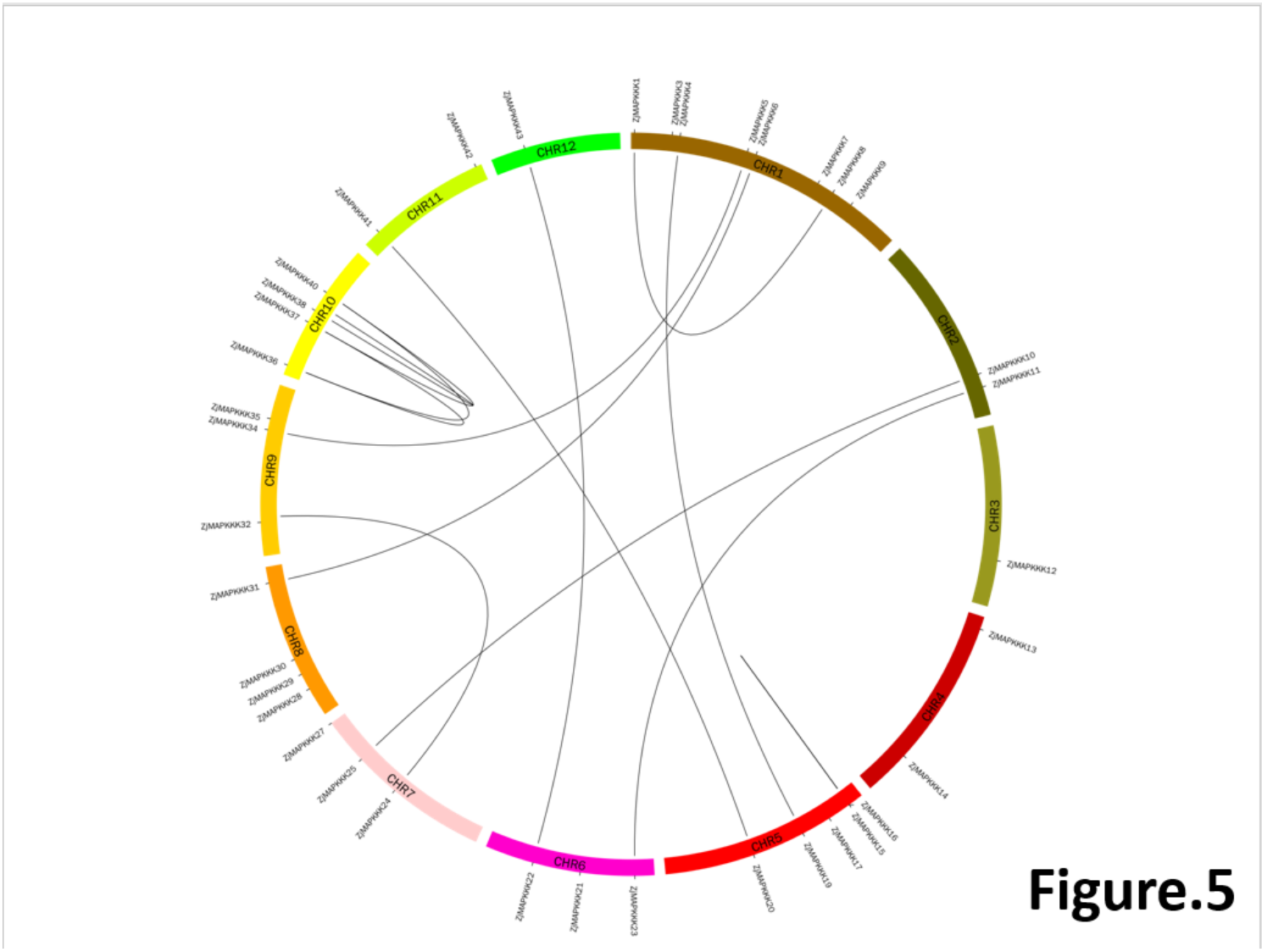

Figure 5

Synteny analysis of ZjMAPKKK genes in the Chinese jujube genome. The black lines indicate duplicated ZjMAPKKK gene pairs.

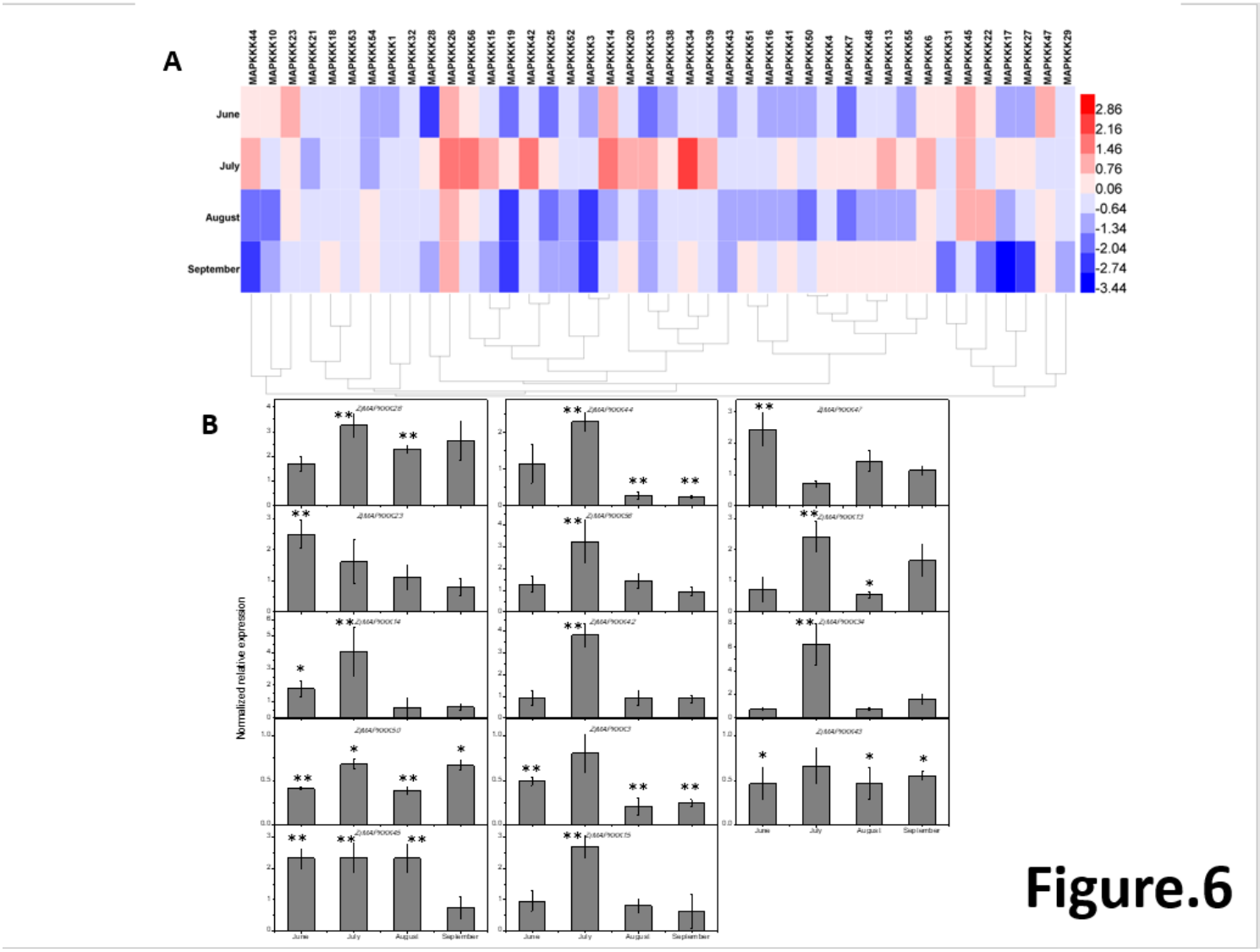

Figure.6

Figure 6

Relative expression profiles of ZjMAPKKKs in jujube witch broom leaves from June to September. The expression levels of ZjMAPKKKs in the leaves of healthy trees were used as a control. (A) Heat map analysis of the ZjMAPKKKs based on the log2-based fold-change values. (B) The relative expression levels of the representative members of ZjMAPKKKs in three independent replications (the error bar represents standard deviation, SD). Asterisks indicate the corresponding genes significantly up- or downregulated at each time within symptomatic leaves compared with healthy control leaves (*P < 0.05, **P < 0.01).

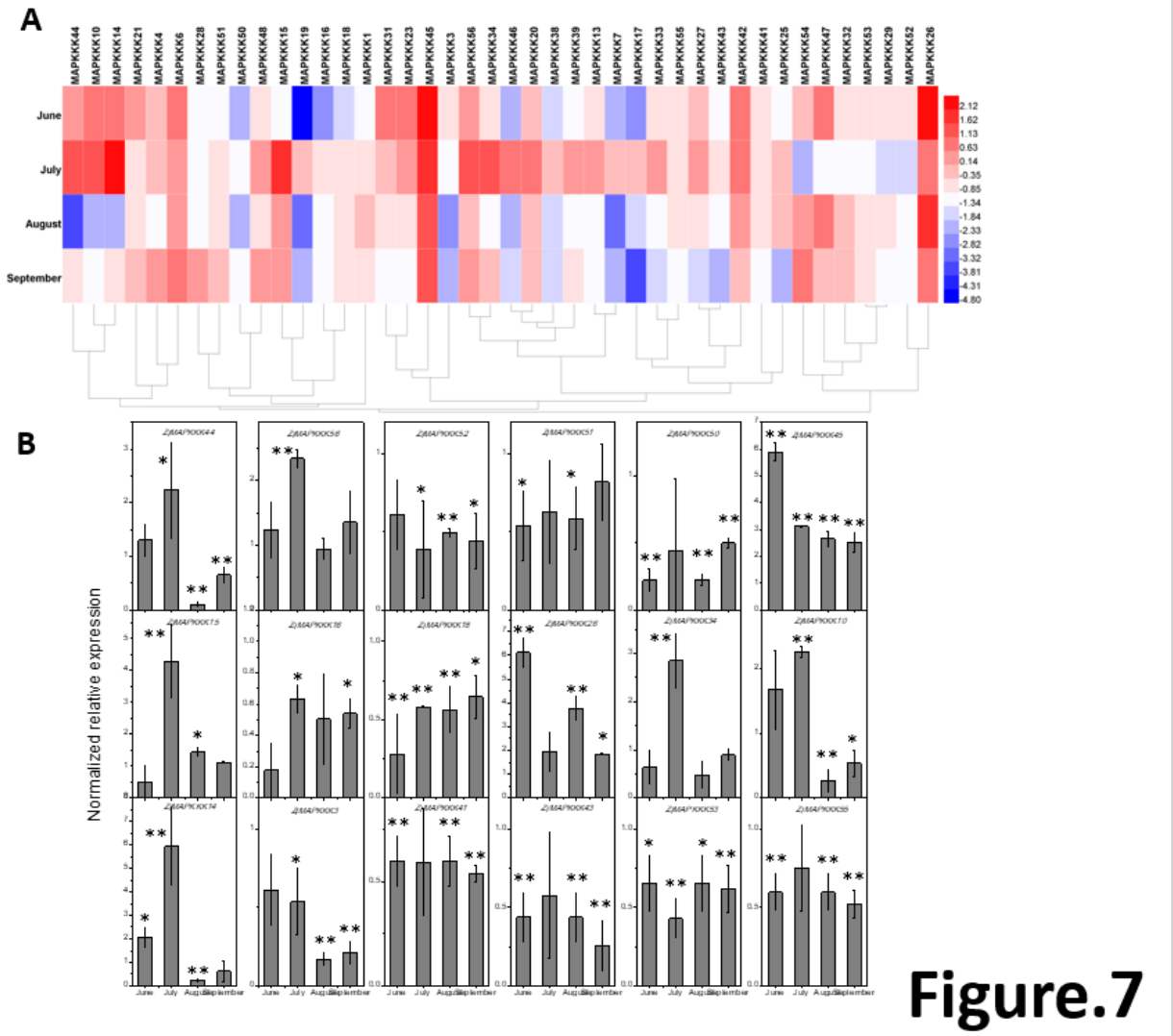

Figure.7

Figure 7

Relative expression profiles of ZjMAPKKKs in phyllody leaves from June to September. The expression levels of ZjMAPKKKs in the leaves of healthy trees were used as a control. (A) Heat map analysis of the ZjMAPKKKs based on the log2-based fold-change values. (B) The relative expression levels of representative members of ZjMAPKKKs in three independent replications (the error bar represents standard deviation, SD). Asterisks indicate the corresponding genes significantly up- or downregulated at each time in symptomatic leaves compared with healthy control leaves (*P < 0.05, **P < 0.01).

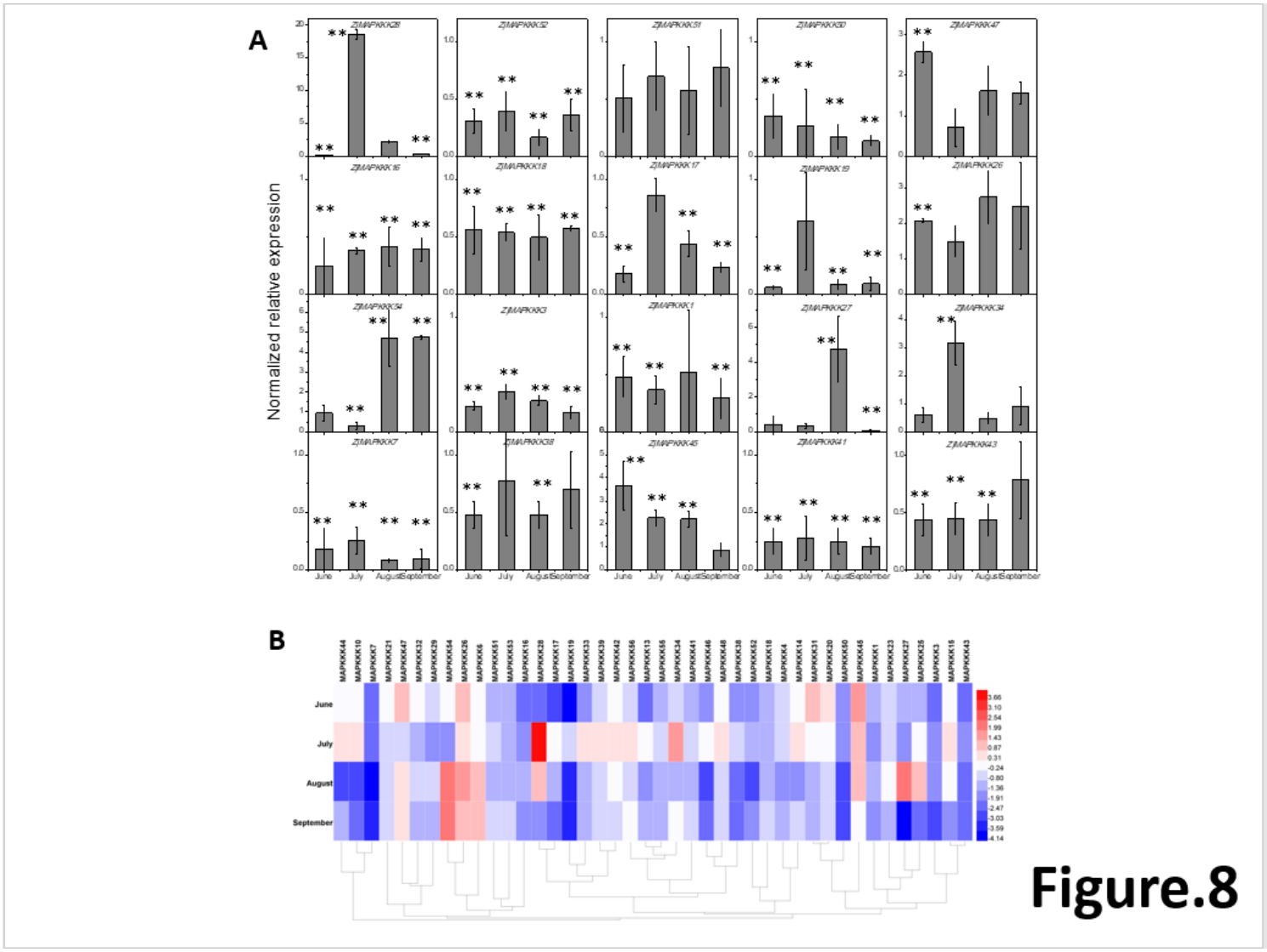

Figure 8

Relative expression profiles of ZjMAPKKKs in apparently normal (but infected) leaves from June to September. The expression levels of ZjMAPKKKs in the leaves of healthy trees were used as a control. (A) The relative expression levels of representative members of ZjMAPKKKs in three independent replications (the error bar represents standard deviation, SD). (B) Heat map analysis of the ZjMAPKKKs based on the log2-based fold-change values. Asterisks indicate the corresponding genes significantly up- or downregulated at each time within symptomatic leaves compared with healthy control leaves (*P < 0.05, **P < 0.01).

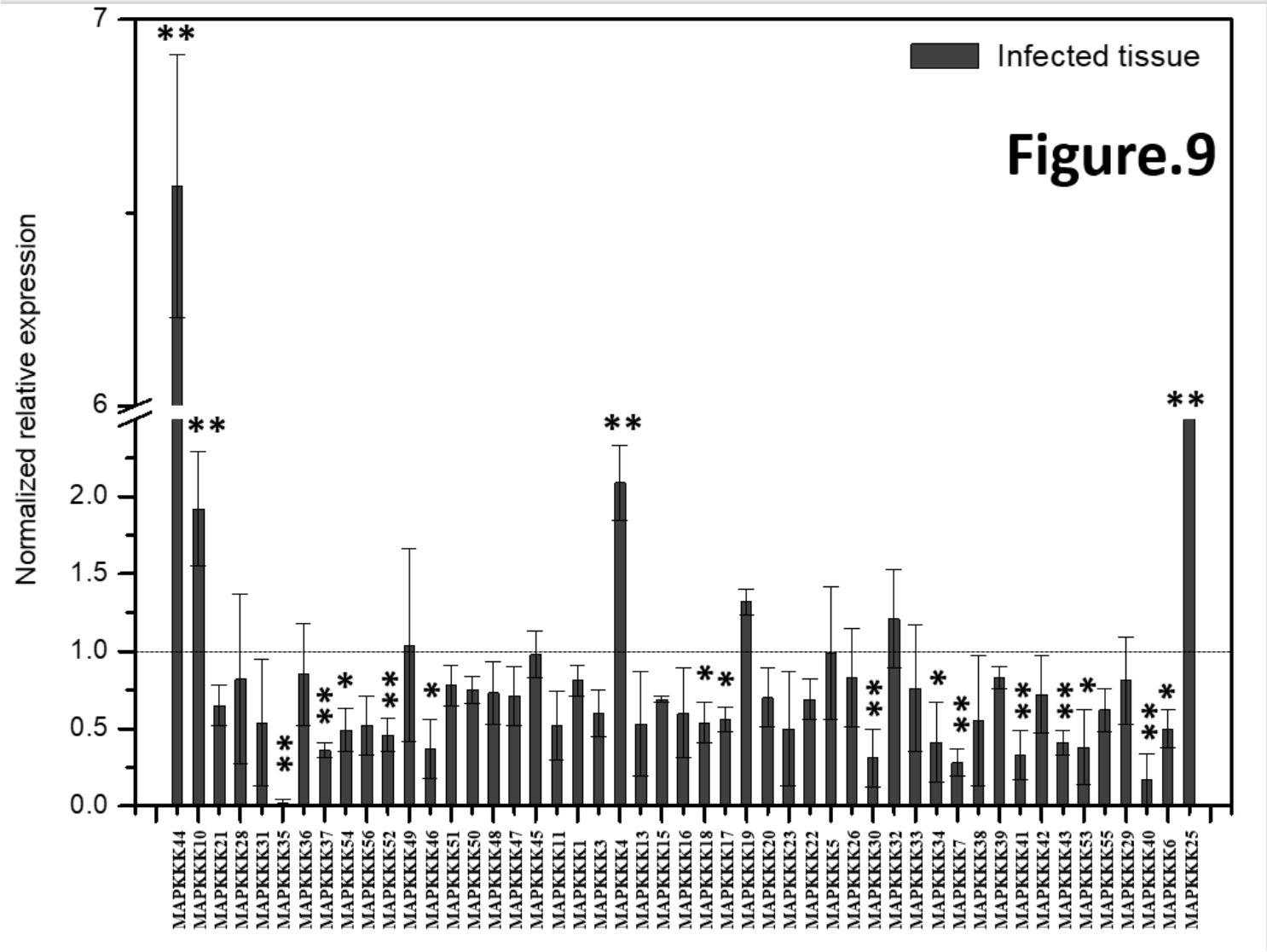

Figure 9

Expression profiles of ZjMAPKKKs in phytoplasma diseased plantlets and healthy tissue in in vitro cultured plantlets. Healthy plantlets were used as controls. Three independent replications were carried out (the error bar represents a standard deviation, SD). Asterisks indicate the corresponding genes significantly up- or downregulated at each time within symptomatic leaves compared with healthy control leaves (*P < 0.05, **P < 0.01).

Supplementary Files

This is a list of supplementary files associated with this preprint. Click to download.

- Additionalfile6TableS2.xls
- Additionalfile8TableS3.xls
- Additionalfile3Fig.S2.docx
- Additionalfile7Fig.S5.pdf

- Additionalfile4Fig.S3.docx
- Additionalfile9TableS4.xls
- Additionalfile5Fig.S4.docx
- Additionalfile2TableS1.xls
- Additionalfile1Fig.S1.pdf